Conformational Stabilization of 1,3-Benzodioxole: Anomeric Effect by Natural Bond Orbital Analysis

Seongho Moon and Younghi Kwon

Department of Chemistry, Hanyang University, Seoul 133-791, Korea

Jaebum Lee and Jaebum Choo*

Department of Chemistry, Hanyang University, Ansan 425-791, Korea

Received: December 10, 1999; In Final Form: January 17, 2001

The conformation of 1,3-benzodioxole has been examined using ab initio calculation and natural bond orbital (NBO) analysis in order to find the origin of its unusual nonplanarity. Geometry optimizations for the planar (C_{2v}) and flap-puckered (C_s) conformers of 1,3-benzodioxole have been performed at the HF, B3LYP, and MP2 levels, and the results indicate that the flap-puckerd conformer is more stable than the planar conformer. High-level electron correlation treatments with extended basis sets have also been performed to provide a reliable prediction of the puckering barrier for 1,3-benzodioxole. The calculated puckering barrier appears to be in reasonable agreement with the experiment, but the divergent behavior of the Møller−Plesset series suggests that it is impossible with conventional basis sets smaller than 400 functions to converge the barrier height. NBO analysis of the Hartree−Fock wave functions shows that the conformational preference of the C_s conformer over the C_{2v} is the result of a wide variety of hyperconjugative orbital interactions, but the interaction between the oxygen lone pair (n_p) and the σ^*_{CO} orbital, which is closely associated with the anomeric effect, is the most important factor favoring the nonplanar conformation. However, 1,3-benzodioxole has a lower puckering barrier to planarity than 1,3-dioxole due to the suppression of the anomeric effect by the benzene ring.

Introduction

It has long been known that the relative balance between two opposing forces determines the equilibrium conformation of cyclopentene (I). Ring angle strain tends to keep the ring planar, whereas torsional strain, caused by CH_2-CH_2 interactions, tends to pucker the ring. Far-infrared and Raman spectroscopy have been extensively used to study the ring-puckering vibration of cyclopentene.[1,2] The previously reported experimental results show that cyclopentene has a puckered structure with a barrier of 0.66 kcal/mol[3] because torsional interactions are minimized when the hydrogen atoms of adjacent methylene groups become staggered. A high-level ab initio calculation[4] has been performed to ascertain the puckered equilibrium structure of cyclopentene, and the calculated results were very consistent with the experimental values.

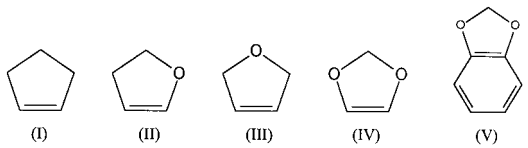

For 2,3-dihydrofuran (II) the barrier to planarity is decreased to 0.24 kcal/mol[5] since only one CH_2-CH_2 torsional interaction exists in this molecule. On the other hand, 2,5-dihydrofuran (III) is planar[6] since there are no torsional forces to pucker the molecule. 1,3-Dioxole (IV) was expected to be planar since it has no adjacent CH_2 groups. However, the reported gas-phase infrared and Raman results[7] clearly show that the equilibrium structure of molecule IV is puckered with a barrier of 0.79 kcal/mol. In this work, Laane and co-workers reasoned that this unexpected nonplanarity of IV must be attributed to the anomeric effect which is present in molecules with O−C−O linkages. Sordo and co-workers[8] carried out high-level ab initio calculation and natural bond orbital (NBO) analysis to support such a conclusion. Their MP4/6-31G(d,p)//MP2/6-31G(d,p) calculation was able to provide a satisfactory prediction of the puckering barrier of IV. Furthermore, their NBO analysis showed that the $n \rightarrow \sigma^*$ orbital interactions involving the oxygen lone pairs and the C−O vacant antibonding orbital (Figure 1) play a decisive role in explaining the above-mentioned experimental results. On the basis of both the experimental and theoretical results for IV, the anomeric effect has been recognized as having much broader relevance to conformational processes of ring molecules, even though it was first identified as an anomalous effect on sugar conformations.[9]

Recently, conformational studies have been extended to 1,3-benzodioxole (V) in order to determine the influence of the benzene ring on the anomeric effect.[10,11] Sakurai et al.[11] determined a two-dimensional potential energy surface in terms of ring-puckering and ring-flapping coordinates from the far-infrared and Raman spectra of V. It was determined that the molecule has a barrier to planarity of 164 cm^{-1} (0.47 kcal/mol) and energy minima at puckering and flapping angles of $\pm 24°$ and $\mp 3°$, respectively. The barrier for V is considerably lower than the barrier of 275 cm^{-1} (0.79 kcal/mol) determined for IV, reflecting a suppression of the anomeric effect by the benzene ring.

To gain more insight into the diminished anomeric effect on V, we undertook a theoretical investigation of this molecule using ab initio calculation and NBO analysis. The planar (C_{2v}) and flap-puckered (C_s) structures of V have been optimized

* Corresponding author. E-mail: jbchoo@email.hanyang.ac.kr.

10.1021/jp994354s CCC: $20.00
Published on Web 03/01/2001

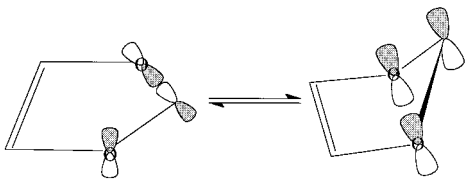

Figure 1. n→σ* orbital interactions involved in the anomeric effect for planar and puckered conformations of 1,3-dioxole.

using HF, B3LYP, and MP2 levels with the 6-31G(d) basis set, and then high-level electron correlation treatments with extended basis sets have been carried out to predict a reliable puckering barrier. In addition, the NBO analysis[12−14] has also been carried out to understand the orbital interactions that determine the conformational preference of V. The conformational energies around the C−O bonds can be decomposed using the NBO method, which allows the calculation of the hyperconjugative energy contributions to the total conformational energy. In this way, one obtains the main orbital interactions to contribute to the conformational stabilization of V.

It is the aim of this paper to present a quantum mechanically determined equilibrium structure as well as to explain the theoretical basis for the conformational preference of 1,3-benzodioxole.

Computations. The molecular orbital energy calculations were carried out using the GAUSSIAN 98 program package.[15] The geometries of the C_s and C_{2v} conformers and the energy barrier to planarity for 1,3-benzodioxole have been calculated at the HF, B3LYP, and MP2 levels with the 6-31G(d) basis set. The single-point energy calculations with larger basis sets and with MP4 correlation treatments at the respective HF/6-31G(d) geometries have also been performed to predict a reliable barrier height. The ring-puckering potential energy profiles have also been determined by specifying the dihedral angle C−O−O−C of the five-membered ring, while all other parameters are optimized.

Natural bond orbital (NBO) analysis at the HF/6-31G(d) level was carried out to understand some of the factors contributing to the total conformational energy. With the NBO deletion procedure, the energy of the hyperconjugative interaction of interest was evaluated by calculating the change in the sum of the energies of occupied orbitals upon deletion of specific off-diagonal elements of the Fock matrix in the NBO basis. In this way, the total energy was decomposed into components associated with covalent and noncovalent contributions, and therefore, the delocalization effects were estimated from comparison of the deletion energies. The NBO method has been known to be a very useful tool in analyzing the type of interactions involved in the anomeric effect.[12−14]

Results and Discussion

Molecular Geometry of 1,3-Benzodioxole. The numbering of the atoms in 1,3-benzodioxole is depicted in Figure 2. The optimized geometries of 1,3-benzodioxole with the HF, MP2, and B3LYP methods are listed in Table 1. Previously reported structural parameters determined by microwave spectroscopy[10] are also included for comparison. The bond lengths calculated at the HF level are obviously underestimated, whereas the inclusion of electron correlation at the MP2 level makes them closer to the microwave data. The overall structural parameters at the B3LYP level are close to the MP2 results and represent definite improvements on the HF results. On the other hand, the puckering and flapping angles calculated at the MP2 level agree better with the microwave data than those obtained from

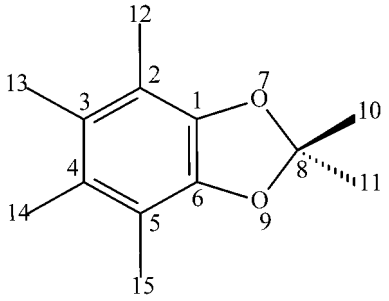

Figure 2. Atom numbering of 1,3-benzodioxole.

TABLE 1: Structural Parameters and Rotational Constants of 1,3-Benzodioxole

structural parameters	HF/6-31G*	B3LYP/6-31G*	MP2/6-31G*	microwave[a]
C_1-C_2	1.366	1.380	1.383	1.387
C_2-C_3	1.401	1.408	1.405	1.400
C_3-C_4	1.380	1.394	1.398	1.395
C_1-C_6	1.382	1.394	1.394	1.400
C_1-O_7	1.358	1.376	1.381	1.368
O_7-C_8	1.407	1.432	1.434	1.432
C_2-H_{12}	1.074	1.085	1.085	1.078
C_3-H_{13}	1.074	1.086	1.087	1.078
C_8-H_{10}	1.083	1.100	1.099	1.094
C_8-H_{11}	1.078	1.094	1.089	1.094
$C_1-C_2-C_3$	116.73	116.74	116.45	118.8
$C_2-C_1-C_6$	122.05	121.98	122.12	120.7
$C_2-C_3-C_4$	121.22	121.29	121.44	120.5
$C_6-C_1-O_7$	109.03	109.62	109.50	110.9
$C_1-O_7-C_8$	106.40	105.60	103.57	−
$O_7-C_8-O_9$	107.36	108.09	107.69	−
$H_{10}-C_8-H_{11}$	110.90	110.91	111.87	−
φ^b	0.9	1.1	2.2	8.28
τ^c	13.0	12.4	25.0	26.81

rotational constants (MHz)	HF/6-31G*	B3LYP/6-31G*	MP2/6-31G*	microwave[a]
A	3900.14 (2.77)[d]	3801.48 (0.17)	3770.59 (−0.64)	3795.05
B	1639.62 (1.13)	1609.57 (−0.73)	1619.91 (−0.09)	1621.33
C	1164.51 (1.48)	1140.51 (−0.61)	1147.08 (−0.61)	1147.54

[a] Ref 10. [b] Ring-flapping angle of five-membered ring ($C_2C_1C_6O_9$). [c] Ring-puckering angle of five-membered ring ($C_1O_7O_9C_8$). [d] Numbers in parentheses indicate percentage differences of theory minus experiment.

the HF and B3LYP levels. The calculated rotational constants are also compared with the experimental values in Table 1. It is seen that the rotational constants calculated at the MP2 level most correctly predict the observed ones. On the basis of the comparison between our computational results and microwave data, we have concluded that the ab initio calculation at the MP2/6-31G(d) level reasonably reproduces the experimental structural parameters of 1,3-benzodioxole.

Barrier to Planarity of 1,3-Benzodioxole. Recently, Sakurai et al.[11] reported the two-dimensional vibrational potential energy surface of 1,3-benzodioxole from the analysis of the far-infrared and Raman spectra. This surface shows that the ring-puckering and ring-flapping modes are coupled to each other and that the molecule has a puckered form with a barrier to planarity of 164 cm^{-1}. To obtain a more reliable two-dimensional potential energy surface, they first determined a one-dimensional ring-puckering potential energy function. In the case of the one-dimensional model, the agreement between observed and calculated transitional values was not bad, but it was worse for the higher transitions.[11] Moreover, the one-dimensional model could not explain the large change in frequency separations in the flapping excited states. Thus, they determined a two-

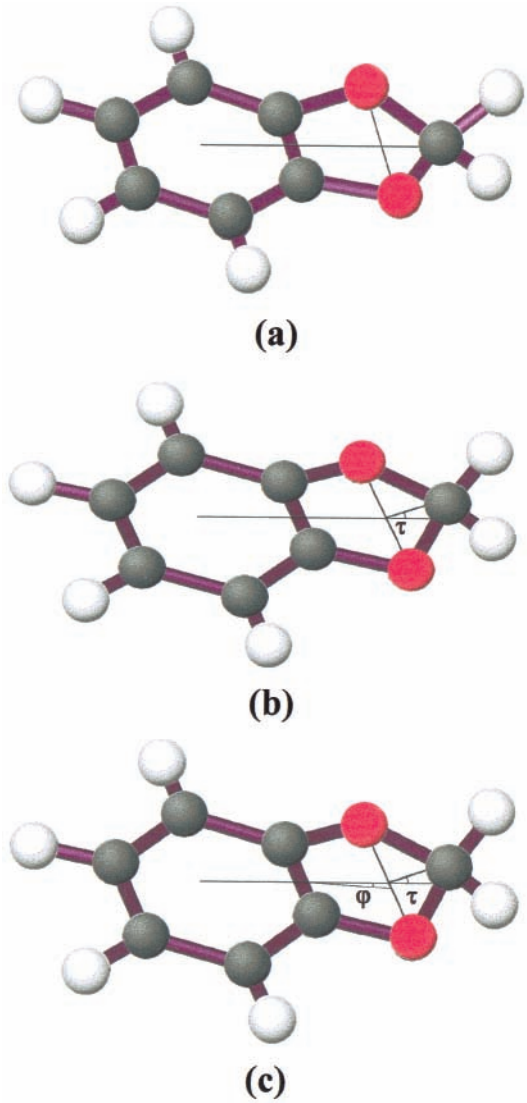

Figure 3. Conformational structures corresponding to (a) planar, (b) planar-puckered, and (c) flap-puckered for 1,3-benzodioxole. Puckering (τ) and flapping (φ) angles are also indicated.

dimensional potential energy surface in order to consider the interaction between the ring-puckering and ring-flapping states.[11]

We also performed the ab initio calculations for both the one-dimensional and two-dimensional models. In the one-dimensional model, the flapping dihedral angle $C_2C_1C_6O_9$ was fixed at 180°, and only the ring-puckering motion of the five-membered ring was considered. We label this one-dimensional equilibrium structure the "planar-puckered" form (Figure 3b). The calculated barriers at the HF/6-31G(d), B3LYP/6-31G(d), and MP2/6-31G(d) levels are compared with the experimental value in Table 2. As shown in the table, the HF and B3LYP methods with the basis set 6-31G(d) obviously underestimate the barrier to planarity of 1,3-benzodioxole. On the other hand, the calculated barrier at the MP2/6-31G(d) level (145 cm^{-1}) is close to the experimental one-dimensional barrier of 127 cm^{-1}.[10]

To get a more accurate puckering barrier, we fully optimized the molecular geometry of 1,3-benzodioxole without any geometrical restrictions. The calculated results indicate that the two rings are slightly flapped, and we labeled this model the "flap-puckered" form (Figure 3(c)). All the geometries for the planar (C_{2v}) and flap-puckered (C_s) forms to calculate the puckering barrier heights were optimized with the 6-31G(d) basis set. To judge the accuracy of the puckering barrier, we

TABLE 2: Energy Barriers to Planarity and Dihedral Angles of 1,3-Benzodioxole

	dihedral angle (deg)		energy barrier	
	$C_1O_7O_9C_8$	$C_2C_1C_6O_9$	(cm^{-1})	ref
Experimental				
far-infrared				
planar-puckered[a]	21	180	127	11
flap-puckered[b]	24	−3	164	11
microwave				
flap-puckered	26.8	8.3	126	10
Theoretical				
HF/6-31G*				
planar-puckered	12.2	180	11	this work
flap-puckered	13.0	−0.9	13	this work
B3LYP/6-31G*				
planar-puckered	9.4	180	4	this work
flap-puckered	12.4	−1.1	10	this work
MP2/6-31G*				
planar-puckered	23.5	180	145	this work
flap-puckered	25.0	−2.2	171	this work

[a] One-dimensional potential energy function in terms of ring-puckering coordinate with no flapping allowed. [b] Two-dimensional potential energy surface in terms of ring-puckering and ring-flapping coordinates.

TABLE 3: Calculated Ring-Puckering Barrier Heights of 1,3-Benzodioxole Using Several Basis Sets[a]

basis set	BF[b]	HF[c]	B3LYP[d]	MP2[e]	MP3[e]	MP4[e]
6-31G(d)	147	14.2	10.1	170.6	88.8	140.5
6-31G(d,p)	165	13.1	16.3	165.7	82.8	133.9
6-311G(d)	180	33.9	30.5	312.9	214.4	283.7
6-311G(d,p)	198	34.8	31.1	325.2	224.2	293.5
6-311G(2d,p)	243	13.8	14.1	130.2	46.8	103.1
6-311G(2df,2pd)	354	13.8	13.5	144.3	–	–
6-311G(3df,3pd)	417	14.3	18.4	180.0	–	–
cc-pVDZ	156	20.2	25.9	211.3	123.4	175.0
cc-pVTZ	354	20.8	20.8	183.9	–	–
cc-pVQZ	675	17.6	18.2	–	–	–

[a] Energies in cm^{-1}. [b] Number of basis functions. [c] Single-point energy calculations performed at the respective HF(full)/6-31G(d) geometry. [d] Single-point energy calculations performed at the respective B3LYP(full)/6-31G(d) geometry. [e] Single-point energy calculations performed at the respective MP2(full)/6-31G(d) geometry.

also performed single-point energy calculations with basis sets much larger than 6-31G(d) and with post-MP2 correlation treatments. The results are summarized in Table 3. Similar to the case for the one-dimensional model, the HF and B3LYP calculations for the two-dimensional model underestimate the puckering barrier, and the expansion of the basis set does not alter the barrier more than 20 cm^{-1} in either case.

The electron correlation at the MP2 level substantially increases the calculated barrier height. However, addition of basis functions leads in some cases to divergent behavior of the MP2 series. It is clear from the large MP2 variations that the puckering barriers calculated at the MP2/6-31G(d) and MP2/6-31G(d,p) levels are not reliable due to the deficiency of extra sp basis function. Indeed, the MP2 barrier at the 6-311G(d,p) level is twice as large as two analogous values calculated at the 6-31G(d) and 6-31G(d,p) levels. Thus, these cannot be fully converged values. The inclusion of the 2d function yields a 6-311G(2d,p) MP2 prediction of 130.2 cm^{-1}, whereas further additions of extra valence functions yield a 6-311G(2df,2pd) MP2 barrier of 144.3 cm^{-1} and a 6-311(3df,3pd) MP2 barrier of 180.0 cm^{-1}, respectively. MP2 calculations with the correlation consistent valence double-ζ (cc-pVDZ) and triple-ζ (cc-pVTZ) basis sets have also been performed, and the calculated puckering barriers are 211.3 and 183.9 cm^{-1}, respectively. The MP4 calculations with several basis sets were also performed.

The computed barrier heights, from 6-31G(d) to 6-311G(2d,p) basis sets at the MP4 level, are observed to oscillate as before, but the cc-PVDZ MP4 value of 175.0 cm^{-1} is very close to the 6-311G(3df, 3pd) and cc-pVTZ MP2 values. On the basis of our MP2 and MP4 calculations with larger basis sets, the final theoretical proposal for the ring-puckering barrier is estimated to be 175 ± 50 cm^{-1}, even though the barrier height at the basis set limit could not be estimated due to the limited computer CPU time. This barrier appears to be in reasonable agreement with experimental value of 164 cm^{-1}. However, the divergent behavior of the MP series in Table 3 suggests that it is impossible with conventional basis sets smaller than 400 functions to converge the barrier height.

In the far-infrared analysis of 1,3-benzodioxole by Laane et al., the two-dimensional potential energy surface, in terms of ring-puckering and ring-flapping coordinates, shows that the molecule has energy minima at puckering and flapping angles of ±24° and ∓3°, respectively.[11] The lowest-energy flapping conformation corresponds to a saddle point 164 cm^{-1} above the puckering conformation on the potential energy surface. This means that only two global minima exist, (+24°,−3°) and (−24°,+3°), and no local minima exist on their potential energy surface. Our ab initio calculation predicts that the global minima exist at (+25°,−2°) and (−25°,+2°), and the calculated puckering and flapping angles for the global minima agree remarkably well with the experimental values. However, it should be noted that our ab initio potential energy surface predicts two additional shallow local minima at (+25°,+2°) and (−25°,−2°), corresponding to the second lowest flapping conformations 90 cm^{-1} above the global minima. On the basis of both the experimental and computational results, it is clear that the energy of puckering conformations is much lower relative to the flapping energy, but whether the ring-flapping minima actually exist is uncertain.

NBO Analysis of 1,3-Benzodioxole. To investigate the preference of the nonplanar conformer for 1,3-benzodioxole, we have performed an NBO analysis. Figure 4a shows the HF, B3LYP, and MP2 ring-puckering energy profiles. As mentioned above, the HF calculation underestimates the barrier to planarity. The HF method, however, predicts a qualitatively correct double-minimum potential energy profile, even though the role played by electron correlation at the MP2 level is very important to determine the accurate barrier height. Thus, the NBO analysis of HF wave functions is able to properly identify the main driving forces, even though the myriad modulating forces are not precisely balanced at this level, leading to underestimations of the barrier.

On the basis of this energy viewpoint, a series of structures with fixed $C_1O_7O_9C_8$ dihedral angles ranging from 0° to 40° has been optimized at the HF/6-31G(d) level. Following the deletion procedure, we obtained the delocalization energies (ϵ_{del}) and Lewis energies (ϵ_{Lewis}; all energy contributions apart from delocalization effects), and they are plotted in Figure 4b. It is noteworthy that the decrease of ϵ_{del} correlates with decreasing E_{tot} for $C_1O_7O_9C_8$ dihedral angles between 0° to 13°. The increase of ϵ_{Lewis} is compensated by the decrease of ϵ_{del} in this range. Thus, ϵ_{del} is likely to contribute to the stabilization of the puckered form of 1,3-benzodioxole.

To better understand the origin of the main orbital interactions for the negative contribution to total energy, we have decomposed ϵ_{del} into several components around the C−O bonds using the NBO deletion procedure. The six greatest hyperconjugative energy contributions to the energy differences between C_{2v} and C_s structures of 1,3-benzodioxole are summarized in Table 4. It is noteworthy that the deletion energy corresponding to $n_p \rightarrow \sigma^*_{CO}$ interaction, which is commonly associated with the anomeric effect, shows the greatest contribution of 12.5% among all the interaction energies. The other large hyperconjugations favoring the C_s nonplanar form are the $\sigma_{CO} \rightarrow \sigma^*_{CH}$ and $n_s \rightarrow \sigma^*_{CH}$ interactions. Further interactions favoring the C_s nonplanar form are those involving Rydberg NBOs, but they are individually smaller than 5% in absolute value. For example, the two greatest contributions of $n \rightarrow RY_{C*}$ and $\pi^*_{C=C} \rightarrow RY_{C*}$ are 4.3% and 3.6%, respectively. On the contrary, the hyperconjugative interaction between the lone pairs of oxygen atoms and C=C antibonding orbitals of benzene ring ($n_p \rightarrow \pi^*_{C=C}$) is the greatest one favoring the C_{2v} form. The other two interactions, favoring the planar C_{2v} form, are also listed in the table.

Figure 5 shows the change of total hyperconjugative energies and those of four greatest hyperconjugative contributions as a function of the puckering dihedral angle. The hyperconjugative

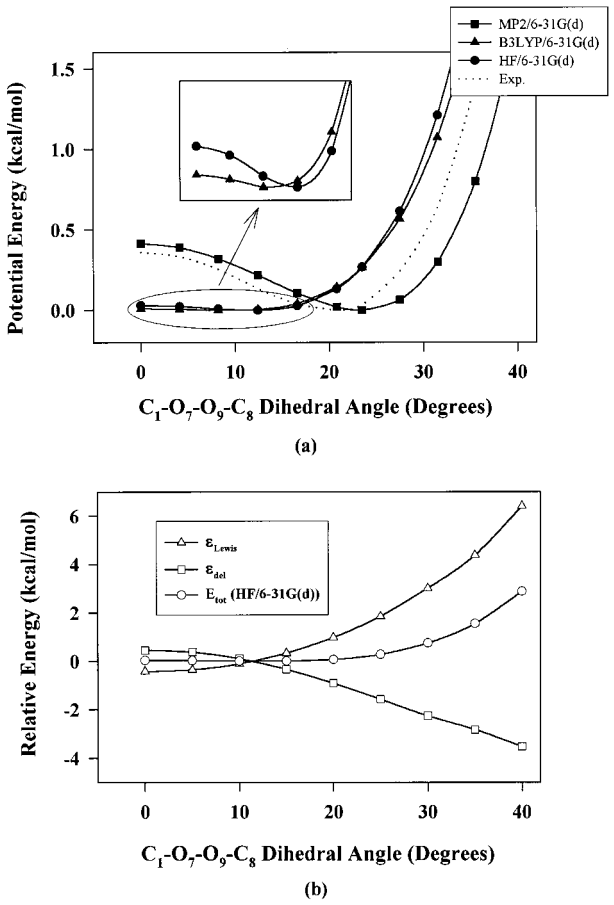

Figure 4. (a) Ring-puckering potential energy curves of 1,3-benzodioxole at the HF, B3LYP, and MP2 levels. (b) Contributions of Lewis energy (ϵ_{Lewis}) and delocalization energy (ϵ_{del}) to total HF/6-31G(d) energy (E_{total}) in 1,3-benzodioxole.

TABLE 4: Analysis of the Hyperconjugatve Contribution (kcal/mol) to the Main Orbital Interaction Energies of C_{2v} and C_s Conformers of 1,3-Benzodioxole

	C_{2v}[a]	C_s[b]	$\Delta(C_{2v}-C_s)$	% contribution
Preference for C_s				
$\epsilon_{OCO}(n_p \rightarrow \sigma^*_{CO})$	0.0	1.20	−1.20	12.5
$\epsilon_{COCH}(\sigma_{CO} \rightarrow \sigma^*_{CH})$	1.20	1.72	−0.52	5.9
$\epsilon_{OCH}(n_s \rightarrow \sigma^*_{CH})$	0.38	0.93	−0.55	5.5
Preference for C_{2v}				
$\epsilon_{OCC}(n_p \rightarrow \pi^*_{C=C})$	39.82	39.00	0.82	8.7
$\epsilon_{OCH}(n_p \rightarrow \sigma^*_{CH})$	21.70	21.16	0.54	5.8
$\epsilon_{OCO}(n_s \rightarrow \sigma^*_{CO})$	10.20	9.74	0.46	4.8

[a] Planar conformation. [b] Puckered conformation.

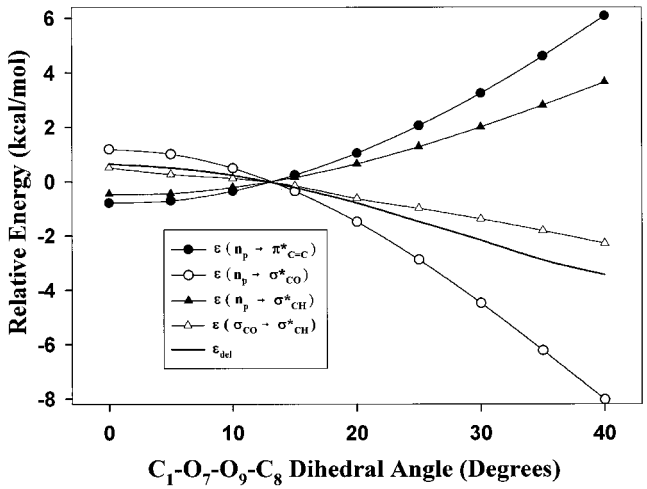

Figure 5. Contributions of $n_p \rightarrow \sigma^*_{CO}$, $n_p \rightarrow \pi^*_{C=C}$, $\sigma_{CO} \rightarrow \sigma^*_{CH}$, and $n_p \rightarrow \sigma^*_{CH}$ interactions to the delocalization energy (ϵ_{del}) of 1,3-benzodioxole.

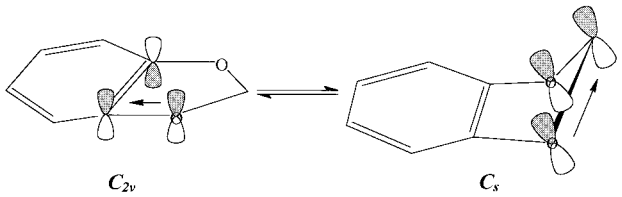

Figure 6. Orientation of the oxygen nonbonding orbitals for (a) planar and **(**b) puckered conformations of 1,3-benzodioxole.

contributions such as $n_p \rightarrow \pi^*_{C=C}$ and $n_p \rightarrow \sigma^*_{CH}$ interactions are increased with increasing dihedral angle, and these contributions are compensated by the opposing effects due to $n_p \rightarrow \sigma^*_{CO}$ and $\sigma_{CO} \rightarrow \sigma^*_{CH}$ interactions. However, the decrease of delocalization energy, ϵ_{del}, is mainly due to negative $n_p \rightarrow \sigma^*_{CO}$ contribution, as shown in Figure 5.

Figure 6 shows the preferred orientation of the oxygen nonbonding orbitals for the two greatest opposing hyperconjugative interactions, $n_p \rightarrow \sigma^*_{CO}$ and $n_p \rightarrow \pi^*_{C=C}$. The oxygen nonbonding orbital, which is perpendicular to the ring, cannot interact with the σ^*_{CO} orbital, which is on the plane of the ring (C_{2v} planar structure in Figure 6). On the other hand, the orbital interaction between the oxygen nonbonding orbital and the $\pi^*_{C=C}$ orbital decreases as the ring puckers up.

The six orbital interaction components in Table 4 give only about 40% of the total hyperconjugation, and the NBO analysis indicates that the conformational preference for the C_s over C_{2v} is the result of rather complicated orbital interactions. Nonetheless, one can conclude that the hyperconjugative $n_p \rightarrow \sigma^*_{CO}$ contribution associated with the anomeric effect is the most important factor in determining the nonplanar equilibrium conformation of 1,3-benzodioxole based on the data in Table 4. The $n_p \rightarrow \pi^*_{C=C}$ contribution which prefers the planar conformation is compensated by the opposing effects due to the $n_p \rightarrow \sigma^*_{CO}$ interaction. These effects mainly provide the conformational stabilization of the puckered structure in 1,3-benzodioxole. However, 1,3-benzodioxole has a lower barrier to planarity than 1,3-dioxole due to the stronger $n_p \rightarrow \pi^*_{C=C}$ influence of the benzene ring on the anomeric effect. This is also the conclusion which was drawn from the experimental work.[11]

Conclusions

In the present study, the ring-puckering conformation and the origin of the anomeric effect in 1,3-benzodioxole have been examined by the ab initio calculation and by NBO analysis. High-level electron correlation treatments with extended basis sets have also been performed to provide a reliable prediction of the puckering barrier for 1,3-benzodioxole. The calculated puckering barrier appears to be in reasonable agreement with the experiment, but the divergent behavior of the MP series suggests that it is impossible with conventional basis sets smaller than 400 functions to converge the barrier height.

The NBO analysis at the HF/6-31G(d) level indicates that the conformational preference of 1,3-benzodioxole for the C_s over the C_{2v} structure is the result of a wide variety of orbital interactions. However, the hyperconjugation effect, caused by the $n_p \rightarrow \sigma^*_{CO}$ orbital interaction, is one of the most important factors for stabilizing the puckered equilibrium conformation of 1,3-benzodioxole. There are other interactions favoring the C_s nonplanar structure, but they are individually smaller than the $n_p \rightarrow \sigma^*_{CO}$ interaction. The $n_p \rightarrow \sigma^*_{CO}$ interaction increases as the ring puckers up; a planar ring molecule cannot have any anomeric interaction. Therefore, the $n_p \rightarrow \pi^*_{C=C}$ contribution which prefers the planar conformation is compensated by the opposing effect due to the $n_p \rightarrow \sigma^*_{CO}$ interaction. These effects provide the conformational stabilization of the puckered structure in 1,3-benzodioxole.

Acknowledgment. This work was supported by Korea Research Foundation Grant (KRF-99-DI0053).

References and Notes

(1) (a) Laane, J. *Pure Appl. Chem.* **1987**, *59*, 1307. (b) Laane, J.; Dakkouri, M.; van der Veken, B; Oberhammer, H. *Structures and Conformations of Non-Rigid Molecules*; NATO ASI Series; Kluwer Academic Publisher: Dordrecht, The Netherlands, 1993. (c) Laane, J. *Annu. Rev. Phys. Chem.* **1994**, *45*, 197. (d) Laane, J. *Int. Rev. Phys. Chem.* **1999**, *18*, 301.

(2) Laane, J. *J. Phys. Chem. A* **2000**, *104*, 7715.

(3) (a) Villarreal, J; Bauman, L. E.; Laane, J. *J. Phys. Chem*. **1976**, *80*, 1172. (b) Bauman, L. E.; Killough, P. M.; Cooke, J. M.; Villarreal, J.; Laane, J. *J. Phys.* Chem. **1982**, *86*, 2000. (c) Villarreal, J.; Bauman, L. E.; Laane, J. *J. Chem. Phys*. **1975**, *63*, 3727.

(4) Allen, W. D.; Császár, A. G.; Horner, D. A. *J. Am. Chem. Soc.* **1992**, *114*, 6834.

(5) Green, H. *J. Chem. Phys.* **1969**, *50*, 1619.

(6) (a) Ueda, T.; Shimanouchi, T. *J. Chem. Phys.* **1967**, *47*, 4042. (b) Carreira, L. A.; Mills, I. M.; Person, W. B. *J. Chem. Phys.* **1972**, *56*, 1444.

(7) Cortez, E.; Verastegui, R.; Villarreal, J.; Laane, J. *J. Am. Chem. Soc*. **1993**, *115*, 12132.

(8) Suárez, D.; Sordo, T. L.; Sordo, J. A. *J. Am. Chem. Soc*. **1996**, *118*, 9850.

(9) (a) Tvaroska, I.; Bleha, T. In *Anomeric and Exo-Anomeric Effects in Carbohydrate Chemistry*; Tyson, R. S. Horton, D. Eds.; Academic Press, Inc.: New York, 1989; Vol. 47. (b) Juaristi, E.; Cuevas, G. *The Anomeric Effect*; CRC Press, Inc.: Boca Raton, FL, 1995.

(10) Caminati, W.; Melandri, S.; Corbelli, G.; Favero, L. B.; Meyer, R. *Mol. Phys*. **1993**, *80*, 1297.

(11) Sakurai, S.; Meinander, N.; Morris, K.; Laane, J. *J. Am. Chem. Soc*. **1999**, *121*, 5056.

(12) Glendening, E. D.; Reed, A. E.; Carpenter, J. E.; Weinhold, F. *NBO 3.0 Program Manual*; Gaussian Inc.: Pittsburgh, PA, 1995.

(13) Reed, A. E.; Curtiss, L. A.; Weinhold, F. *Chem. Rev.* **1988**, *88*, 899.

(14) Salzner, U.; Schleyer, P. *J. Am. Chem. Soc*. **1993**, *115*, 10231.

(15) Frisch, M. J.; Trucks, G. W.; Schlegel, H. B.; Scuseria, G. E.; Robb, M. A.; Cheeseman, J. R.; Zakrzewski, V. G.; Montgomery, J. A.; Stratmann, R. E.; Burant, J. C.; Dapprich, S.; Millam, J. M.; Daniels, A. D.; Kudin, K. N.; Strain, M. C.; Farkas, O.; Tomasi, J.; Barone, V.; Cossi, M.; Cammi, R.; Mennucci, B.; Pomelli, C.; Adamo, C.; Clliford, S.; Ochterski, J.; Petersson, G. A.; Ayala, P. Y.; Cui, Q.; Morokuma, K.; Malick, D. K.; Rabuck, A. D.; Raghavachari, K.; Foresman, J. B.; Cioslowsski, J.; Ortiz, J. V.; Stefanov, B. B.; Liu, G.; Liashenko, A.; Piskorz, P.; Komaromi, I.; Gomperts, R.; Martin, R. L.; Fox, D. J.; Keith, T.; Al-Laham, M. A.; Peng, C. Y.; Nanayakkara, A.; Gonzalez, C.; Challacombe, M.; Gill, P. M. W.; Johnson, B. G.; Chen, W.; Wong, M. W.; Andres, J. L.; Head-Gordon, M.; Replogle, E. S.; Pople, J. A. *Gaussian 98*, Revision A.7; Gaussian Inc.: Pittsburgh, PA, 1998.